BNL-108511-2015-JA

An In-situ Phosphorus Source for the Synthesis of Cu_3P and the Subsequent Conversion to Cu_3PS_4 Nanoparticle Clusters

Erik J. Sheets
School of Chemical Engineering, Purdue University, 480 Stadium Mall Dr. West Lafayette, Indiana 47907, USA

Wei-Chang Yang
School of Materials Engineering, Purdue University, 701 Stadium Mall Dr. West Lafayette, Indiana 47907, USA

Robert B. Balow
Department of Chemistry, Purdue University, 560 Oval Dr. West Lafayette, Indiana 47907, USA

Yunjie Wang and Bryce C. Walker
School of Chemical Engineering, Purdue University, 480 Stadium Mall Dr. West Lafayette, Indiana 47907, USA

Eric A. Stach[a)]
Center for Functional Nanomaterials, Brookhaven National Laboratory, 2 Center Street, Upton, NY 11973, USA

Rakesh Agrawal[b)]
School of Chemical Engineering, Purdue University, 480 Stadium Mall Dr. West Lafayette, Indiana 47907, USA

[a)] This author was an editor of this journal during the review and decision stage. For the *JMR* policy on review and publication of manuscripts authored by editors, please refer to http://www.mrs. org/jmr-editor-manuscripts/

[b)] Address all correspondence to this author. Email: agrawalr@purdue.edu

ABSTRACT

The search for alternative earth abundant semiconducting nanocrystals for sustainable energy applications has brought forth the need for nanoscale syntheses beyond bulk synthesis routes. Of particular interest are metal phosphides and derivative I-V-VI chalcogenides including copper phosphide (Cu_3P) and copper thiophosphate (Cu_3PS_4). Herein, we report a one-pot, solution-based synthesis of Cu_3P nanocrystals utilizing an in-situ phosphorus source: phosphorus pentasulfide (P_2S_5) in trioctylphosphine (TOP). By injecting this phosphorus source into a copper solution in oleylamine (OLA), uniform and size controlled Cu_3P nanocrystals with a phosphorous-rich surface are synthesized. The subsequent reaction of the Cu_3P nanocrystals with decomposing thiourea forms nanoscale Cu_3PS_4 particles having p-type conductivity and an effective optical band gap of 2.36 eV. The synthesized Cu_3PS_4 produces a cathodic photocurrent during photoelectrochemical measurements, demonstrating its application as a light-absorbing material. Our process creates opportunities to explore other solution-based metal-phosphorus systems and their subsequent sulfurization for earth abundant, alternative energy materials.

INTRODUCTION

Nanocrystalline transition metal phosphides have attracted attention across several fields for their magnetic,[1] catalytic,[2] and electronic properties.[3] Specifically, copper phosphide (Cu_3P) has become relevant as an alternative anode material in lithium-ion batteries.[4,5] A need to develop simple solution-based synthesis methods that also provide tight physical property control is necessary for this technology to become viable. Previously, Cu_3P and other metal-phosphides have been synthesized by solid-vapor transport,[6] solvothermal

reactions,[7] yellow/white phosphorus,[8,9] and other solution-based methods that utilize the decomposition of trioctylphosphine (TOP).[10–13] Here, we report the synthesis of size tunable Cu_3P nanocrystals by the reaction of copper nanocrystals with a novel solution-based phosphorus source: P_2S_5 in TOP. A hot injection technique was utilized at temperatures between 200 °C and 300 °C to produce nearly uniform Cu_3P nanocrystals.

Extending from Cu_3P, copper thiophosphate (Cu_3PS_4) and copper selenophosphate (Cu_3PSe_4), have recently been reported as having favorable electronic properties for applications as alternative, earth abundant solar absorption materials.[14–16] These ternary chalcogenides have similar crystal structures to CdTe, $Cu(In,Ga)Se_2$, $Cu_2ZnSnSe_4$, as well as Cu_3AsS_4, and it is thus logical to pursue the development of simple and inexpensive syntheses of I-V-VI semiconductors for earth abundant and non-toxic next generation solar devices.[17]

To date, reported syntheses of $Cu_3P(S,Se)_4$ have only been conducted via chemical vapor transport mechanisms.[14,18–21] In this work, we demonstrate nanocrystalline Cu_3P can be used as a precursor to synthesize copper thiophosphate (Cu_3PS_4) in the presence of decomposing thiourea (THU). The resulting p-type Cu_3PS_4 particles have an orthorhombic crystal structure with a wurtzite superstructure,[22] an optical bandgap of 2.36 eV, and a generated stable photoresponse with a current density of 3 $\mu A/cm^2$ under standard AM 1.5G radiation to demonstrate the proof of concept.

EXPERIMENTAL DETAILS

Synthesis of Cu_3P Nanocrystals. A precursor solution containing controlled quantities of P_2S_5 (99%, Sigma Aldrich) and TOP (90%, Sigma Aldrich) was prepared in a round-bottom

flask under nitrogen without further purification. This was stirred at 40 °C for 20 min or until the solution turned homogeneously orange. Oleylamine (OLA) (90%, Sigma Aldrich) was degassed by the freeze-pump-thaw method and stored under inert gas. 10.0 mL OLA was added to 1.5 mmol copper acetylacetonate ($Cu(acac)_2$) (Sigma Aldrich) in a three neck flask under nitrogen and was attached to a standard Schlenk line apparatus and a heating mantle. The copper precursor was heated to reflux under vacuum (120-135 °C), then refilled with argon and evacuated again (repeated 3 times). The Cu-OLA solution was heated rapidly to between 200 °C and 300 °C, then 4.5 mL of the P_2S_5-TOP solution was quickly injected via syringe and a timer was started. Due to the temperature drop of 30-40 °C upon injection, the reaction was heated back to the initial injection temperature and held for 30 min. The flask was cooled naturally to room temperature. The standard reaction consisted of a molar ratio of TOP:P_2S_5:$Cu(acac)_2$ = 10:0.75:1.5 in 10.0 mL OLA.

The Cu_3P particles were washed using a 1:1 (v:v) mixture of toluene (99.5%, Macron Chemicals) and ethanol (200-proof, Koptec) followed by centrifugation at 14 krpm for 5 min in a Beckman Coulter Allegra X-22 centrifuge. The supernatants were decanted and the particles were given a total of 3 additional toluene/ethanol washes before final storage in air or ethanol.

Conversion of Cu_3P to Cu_3PS_4. Nanocrystals of Cu_3P were dried under nitrogen at room temperature and immediately put into a three-neck round-bottom flask with 5 g of thiourea pellets (99%, Sigma Aldrich) providing an excess molar quantity of sulfur. 10 mL of 1-octadecene (90%, Sigma Aldrich) was also added in some experiments at this point, but its presence is not critical for the reaction. The flask was attached to a standard Schlenk line apparatus and evacuated at room temperature. After three cycles of evacuation and refilling with argon, the flask was heated to 180

°C under Argon for at 5 hours before cooling to room temperature. If 1-octadecene was not used, ethanol was injected into the system at <50 °C to aid in collection of the product. The yellow solid was washed by suspending in ethanol and was centrifuged at 14 krpm for 5 min. After discarding the supernatant, the washing process was repeated at least three times before drying under nitrogen.

DISCUSSION

In-situ Copper Nanocrystals. Copper nanocrystals were synthesized by heating copper (II) acetylacetonate ($Cu(acac)_2$) in oleylamine (OLA) at temperatures above 200 °C as previously observed in literature.[23] Immediately prior to the injection of the phosphorus source, P_2S_5 in TOP, aliquots of the $Cu(acac)_2$ precursor in OLA were analyzed for comparison to the targeted product, Cu_3P. Copper nanocrystals were observed to form round clusters whose average diameter grew from 3.8 ± 0.9 nm to 15.0 ± 1.8 nm with increasing reaction temperatures from 200 to 300 °C, respectively. The nanocrystals were uniform and phase pure according to transmission electron microscopy (TEM) and X-ray diffraction (XRD) analysis (see Supplemental Material (SM), FIG. S1).

In-situ Phosphorus Source. TOP is well known to be a strong reducing agent, stabilizer, and solvent.[24] Conversely, P_2S_5 is a strong oxidizing agent and sulfur source. Upon combination of these two species, gas chromatography-mass spectrometry (GC-MS) proved that the phosphorus site on TOP acquired sulfur from P_2S_5, forming trioctylphosphine sulfide (TOPS): a capping agent capable of stabilizing nanocrystals (see SM, FIG. S2).[25] Formation of TOPS suggests phosphorus must be liberated from the P_2S_5 as the sulfur reacts with TOP. Evidence of elemental phosphorus is observed when the solution of P_2S_5 in TOP is heated to 50 °C and a red precipitate forms.

Analysis of the precipitate using energy dispersive X-ray spectroscopy (EDS) in the scanning electron microscope (SEM) revealed a phosphorus to sulfur ratio of 4.8:1, or 12 times the expected ratio of 0.4:1 as in P_2S_5. Further evidence of amorphous red phosphorus was obtained when P_2S_5-TOP was injected into hot OLA (>200 °C) without the presence of copper (otherwise identical conditions to Cu_3P syntheses). Amorphous red phosphorus again formed, with no XRD signature (see SM, FIG. S3) and a molar phosphorus to sulfur ratio greater than 100:1 according to SEM-EDS observations.

Copper Phosphide. The product which resulted from reacting in-situ synthesized copper nanocrystals with the injected solution of TOP and P_2S_5 was characterized by XRD (FIG. 1), TEM (FIG. 2 (a,b)), and SEM-EDS. The XRD pattern for a standard nanocrystalline Cu_3P film (300 °C, Cu:P = 1.5:1) confirmed a hexagonal crystal structure with reference to PDF# 01-071-2261 (P 63 c m (185)). The lattice parameters (a = 6.9106 Å, c = 7.0927 Å) were derived based on the refinement results using both Maud and PowderCell software.

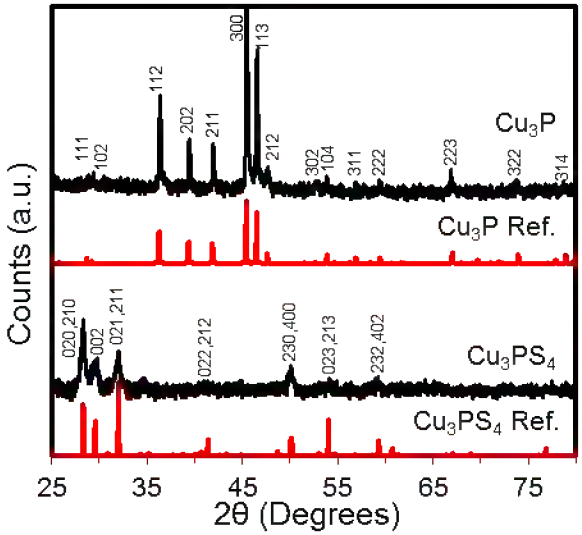

FIG. 1. XRD spectra of Cu_3P synthesized from the in-situ phosphorous source P_2S_5 in TOP (ref. PDF# 01-071-2261). This Cu_3P is reacted with decomposing thiourea to synthesize Cu_3PS_4 also shown (ref. PDF 01-071-3306).

TEM analysis of the standard product indicated that the mean particle diameters ranged from 6.7 nm ± 1.5 nm at 200 °C to 20.8 nm ± 3.3 nm at 300 °C after 30 min (see SM, FIG. S4-6). Particle diameters were independent of reaction times longer than 5 min across similar temperatures. Particles exhibit interplanar spacings consistent with the literature[26] and can be seen in FIG. 2 (b). Unlike other reports of Cu_3P Janus particles,[13] we observe single crystalline nanocrystals through the 200-300 °C temperature range according to high-resolution TEM images.

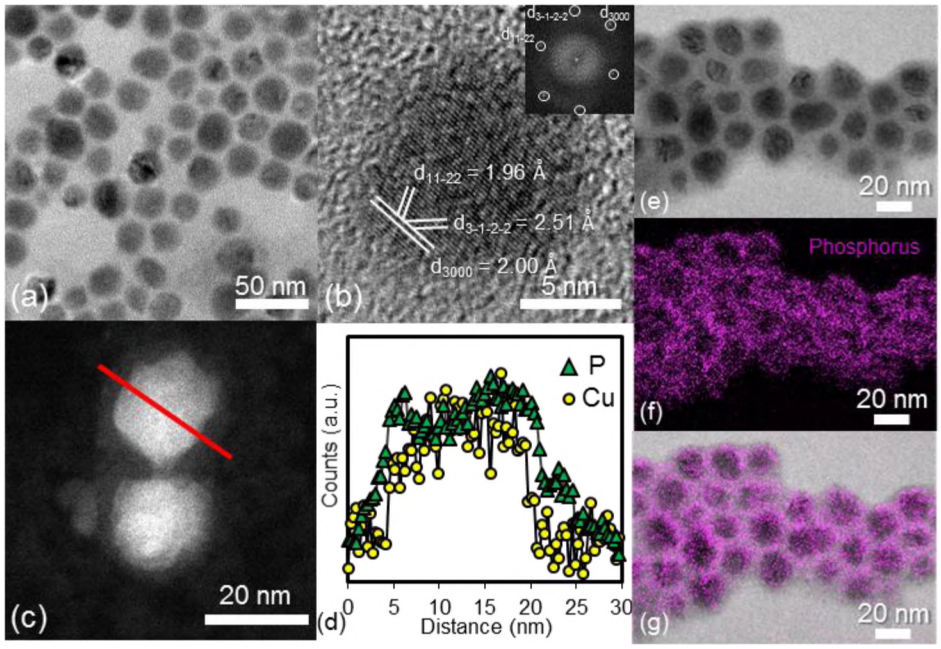

FIG. 2. (a) Bright field and (b) HRTEM images of Cu_3P nanocrystals synthesized by the hot injection of a P_2S_5-TOP solution into a solution charged with $Cu(acac)_2$ in oleylamine. The FFT of (b) is inset. (c) Annular dark field STEM image of two Cu_3P nanocrystals. The solid red line indicates the location of the EELS linescan. (d) STEM EELS linescan showing the precise location of elemental signals for P (green triangles) and Cu (yellow circles) indicating a uniform nanocrystal capped with phosphorus. Note that while the Cu:P ratio is constant within the bulk of the nanoparticle (brightest region), the P signal extends beyond the nanocrystal. (e) Bright field TEM image of Cu_3P nanocrystals with (f) accompanying EFTEM phosphorus map confirming the phosphorus-rich surface. (g) Overlaid EFTEM phosphorus map over the original bright field image.

Analysis of SEM-EDS data for nanocrystals synthesized over various stoichiometric atomic ratios indicated excess phosphorus beyond 3:1 Cu:P. This excess phosphorus was observed to be proportional to the amount of P_2S_5 injected. Conversely, the ratio of Cu:P was independent of the molar amount of TOP present as long as sufficient TOP was provided to remove the sulfur from P_2S_5. When insufficient TOP was used, undesired $Cu_{2-x}S$ was readily formed (see SM, FIG S7). The discrepancy between the XRD showing only one pure phase of Cu_3P and SEM-EDS showing excess phosphorus was hypothesized due to excess amorphous red phosphorus, TOP/TOPS as a surface capping ligand, or a combination of the two. To test this hypothesis, scanning transmission electron microscopy (STEM) and electron energy loss spectroscopy (EELS) linescans were used to show the presence of phosphorus throughout the Cu_3P nanocrystals and identify any variations in phosphorus presence across the nanoparticles as seen in FIG. 2 (c, d). In the STEM EELS linescan, the phosphorus signal was observed to extend beyond the boundary of the copper signal by about 2 nm, while the relative copper and phosphorus signals remained constant across the nanocrystal. Phosphorus mapping using energy-filtered TEM (EFTEM) was employed to detect an increase in phosphorus signal near the edges of the particles, confirming the EELS observation (FIG. 2 (e-g)). Thus, uniform Cu_3P nanocrystals have been synthesized with a phosphorus rich surface caused by either excess amorphous red phosphorus or TOP/TOPS capping ligands which is consistent with literature.[27] An elemental map and linescan of Cu_3P nanocrystals taken using STEM-EDS further confirms uniformity throughout the particles (see SM, FIG. S8, 9).

Multiple reports in the literature have indicated that excess phosphorus is required to achieve phase-pure synthesis of Cu_3P, though the precise amounts have varied

considerably.[7,26] For example, Olofsson reported a homogeneous range with Cu:P ratios between 2.73:1 and 2.82:1 while Aitken et al. report at least a 1:1 ratio for pure phase Cu_3P. Aitken also claims the off-stoichiometry in Cu_3P may either be excess amorphous phosphorus, intrinsic copper vacancies, or a combination there of. De Trizio et al. recently confirmed copper vacancies are thermodynamically favored in this system.[28] We observe that an initial Cu:P ratio of 2.75:1 or greater will result in a copper phase (FIG. 3). At ratios of 2.6:1 and below, only Cu_3P peaks are observed and are found to increase in intensity, accompanied by a slight shift in peak position (FIG. 3 (a)). Although the precise Cu:P ratios determined by SEM EDS varied slightly across experiments, the trend depicts a linear relationship between the amount of phosphorus injected and the final amount of phosphorus observed in the product, as depicted in FIG. 3 (b). Therefore excess phosphorus is needed to obtain phase pure Cu_3P. Notably, the excess phosphorus remains on the outside of the nanocrystal. Efforts to selectively etch the surface phosphorus were unsuccessful.

To illustrate the versatility of P_2S_5 in TOP as an in-situ phosphorus source, InP nanoparticles have also been synthesized in a similar method as Cu_3P. Experimental details and evidence are provided in the SM (FIG. S10).

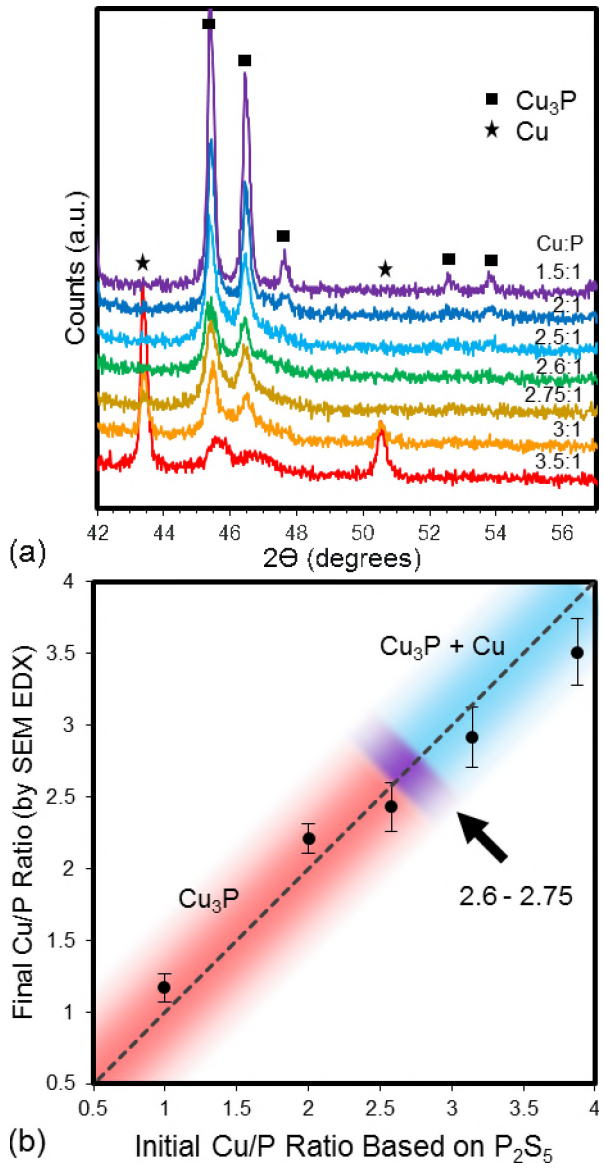

FIG. 3. (a) XRD scans showing the presence of Cu metal (PDF #4-836) with Cu_3P at Cu:P ratios above 2.75:1 and phase-pure Cu_3P at ratios of 2.6:1 and below. (b) Final Cu:P ratios obtained by SEM EDS are found to be dependent on the initial concentration of P_2S_5 in TOP, indicating that excess phosphorus is needed to obtain pure phase Cu_3P.

Copper Thiophosphate. The decomposition of thiourea in the presence of Cu_3P enables the conversion of Cu_3P to Cu_3PS_4. The decomposition of thiourea has been shown to occur in two main steps: the isomerization of thiourea to ammonium thiocyanate followed by decomposition into several gaseous products including ammonia, hydrogen cyanide,

isothiocyanic acid, ammonium cyanamide, and most importantly the sulfide gasses/vapors hydrogen sulfide and carbon disulfide.[29,30] The reaction of sulfur-containing species produced from the decomposition of thiourea with Cu_3P can occur with or without a solvent present at 180 °C. When selecting a solvent, reactions between the solvent and decomposition products were avoided. For example, 1-octadecene proved unreactive and supportive of the conversion reaction while oleylamine formed organic-sulfur complexes without forming Cu_3PS_4.

XRD obtained from a film that was drop cast onto a quartz substrate indicated the formation of the orthorhombic crystal structure of Cu_3PS_4 (FIG. 1). The XRD indicates the presence of only a single phase, with lattice parameters of a = 7.2620 Å, b = 6.3050 Å, and c = 6.0366 Å. SEM EDS data before and after the reaction with thiourea show an increase in sulfur content from Cu:P:S (normal to 3.0 Cu) of 3.0:1.8:0.3 to 3.0:2.6:4.5 (see SM FIG 11, 12). The excess phosphorus from the initial formation of Cu_3P is seen to be present in Cu_3PS_4 coinciding with a large increase in the amount of sulfur present. Non-stoichiometric ratios may also be the result of copper vacancies similar to that which is hypothesized in Cu_3P.[7] Because the EDS was taken for a large area of sample, a more detailed analysis of the individual particles was conducted using TEM techniques.

Synthesis without an additional reaction medium such as 1-octadecene (using only melted thiourea as the solvent and reactant) produced clusters with tube-like pores (see SM, FIG. S11). This indicates a diffusion related mechanism such as the Kirkendall Effect is contributing to the formation of Cu_3PS_4. Synthesis in 1-octadecene produced larger, solid aggregates which were analyzed by TEM (FIG. 4 (a, b)) and STEM EDS (FIG. 4 (c, d)). Aggregates consisted of smaller particles that were not uniform in shape, but were usually

<200 nm. Results of the STEM EDS analysis showed a uniform distribution of Cu, P, and S throughout the particles, confirming that the particles do not have a core-shell structure nor do they have a phosphorus or sulfur rich surface. The counts of characteristic X-ray photons corresponding to Cu, P, and S are expected and observed to increase with thickness of the specimen. Despite the relative noise in the scan, constant ratios of elemental signals across the particles show that the particles are uniform (see SM, FIG. S14). Qualitative atomic ratios across the particles are in agreement with the expected 3:1:4 ratio of Cu:P:S.

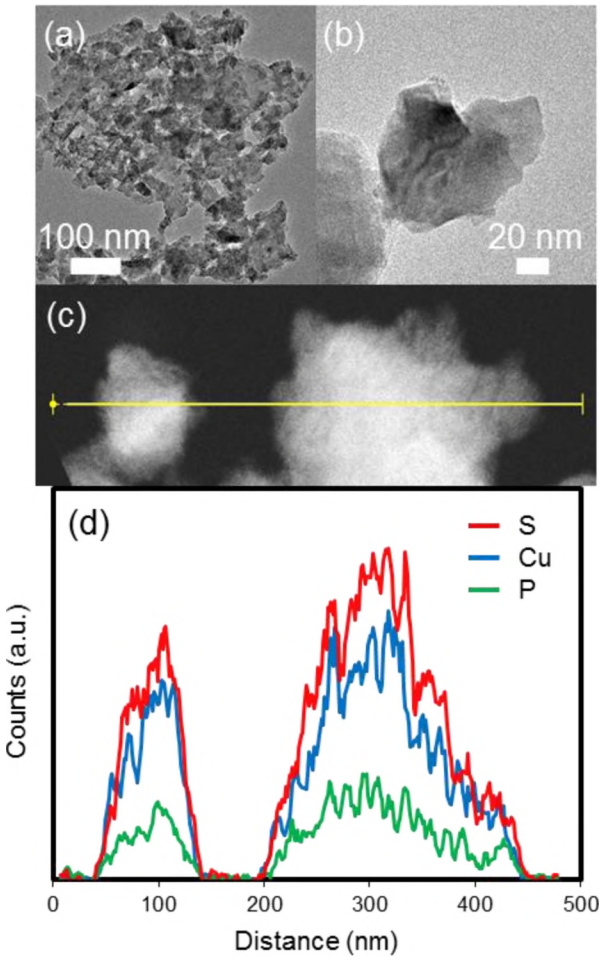

FIG. 4. (a, b) Bright field TEM image of Cu_3PS_4 particles synthesized from the reaction of Cu_3P in 1-octadecene with decomposing thiourea. (c, d) STEM EDS linescan of Cu_3PS_4 showing a uniform atomic composition qualitatively approaching the desired 3:1:4 Cu:P:S ratio. Data represented is a 5-point moving average.

The effective optical bandgap of the Cu_3PS_4 synthesized from thiourea without 1-octadecene was determined by photoluminescence (PL) to be 2.36 eV (525 nm) and is consistent with its yellow color. This peak matches the optical bandgap which matches what we would expect from radiative recombination. The sharpness of PL peaks tends to increase with particle size.[31] Given that some larger particles of Cu_3PS_4 could be present in the analyzed sample, the distribution of particle sizes causes a larger distribution of PL signal. Particularly large crystalline particles likely contribute to the sharpness of the peak at 525 nm in FIG. 5. Our result is also consistent with the previously reported[19] and verified[16] bandgap of 2.38 eV. A wide photoresponse is also observed at a lower energy level centered at 2.19 eV (566 nm). This is potentially caused by a distribution of defect states within the band gap, by the effect of non-uniform particle size distribution, or luminescence of amorphous red phosphorus. The synthesized Cu_3PS_4 was verified as p-type through hot point probe measurements.

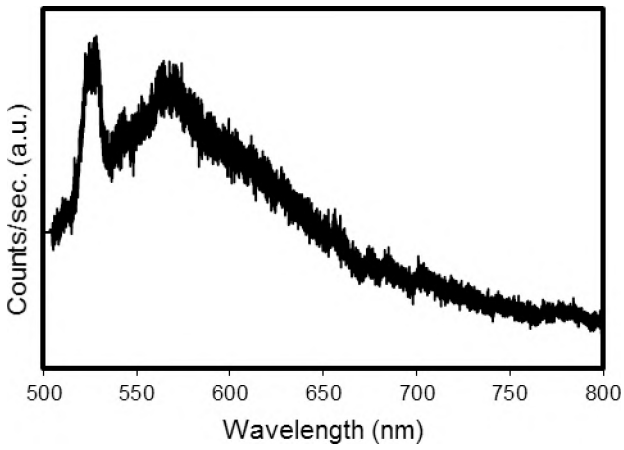

FIG. 5. FIG. 5. Photoluminescence spectrum of Cu_3PS_4 showing the peak photoresponses at 2.36 eV (525 nm) and 2.19 eV (566 nm) near the theoretical optical bandgap of 2.38 eV (521 nm).

Cu_3PS_4 Photoresponse. To demonstrate the application of Cu_3PS_4 as a potential earth abundant solar absorption material, a photoresponse was recorded via photoelectrochemical (PEC) measurements. Cu_3PS_4 photoelectrodes were fabricated by drop casting the Cu_3PS_4 particles suspended in ethanol on an indium doped tin oxide (ITO) substrate and dried in air. The photoelectrodes were then heated in a nitrogen atmosphere for 10 min at 200 °C to help adhere the nanoparticles to the substrate. Photocurrent performance was evaluated in 0.5 M Na_2S (pH 12.0 with HCl) electrolyte with chopped full film illumination through the back of the ITO substrate with solar simulated AM 1.5G light (100 mW/cm^2). FIG. 6 shows the light and dark performance of the Cu_3PS_4 photoelectrodes. At a bias of -1.15 V vs. Ag/AgCl (4 M KCl), the generated cathodic photocurrent increases to a current density of 3 $\mu A/cm^2$ after 600 s. The increasing dark current over time is attributed to the changing equilibrium of the redox couple (S^{2-}/S_n^{2-}) in the electrolyte upon illumination. The photocurrent is stable for 10 min of light/dark cycles without observable photocorrosion. The increased negative current generated when the photoelectrode is illuminated is representative of p-type conductivity. Hot point probe measurements were consistent with this observation. Thus, the Cu_3PS_4 particles produce a stable photoresponse demonstrating its applicability as a solar absorber. An appropriate n-type material is currently being sought for application as a solar device.

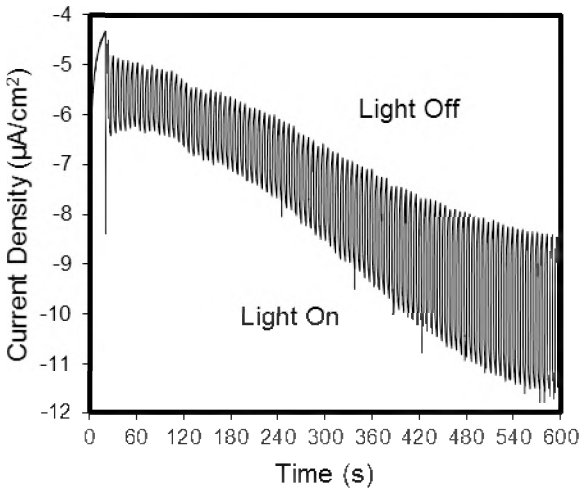

FIG. 6. PEC data collected from back illuminating Cu_3PS_4 on ITO coated soda-lime glass using Na_2S (0.5 M, pH 12.0 with HCl) as the electrolyte with an applied bias of -1.15 V vs. Ag/AgCl (4 M KCl). As the electrolyte equilibrates, the current density stabilizes to 3 $\mu A/cm^2$ after 600 s.

Based on the aforementioned observations, a generalized reaction pathway for the synthesis of Cu_3PS_4 from solution-based precursors is proposed in Scheme 1. The initial reaction of P_2S_5 with TOP induces the formation of TOPS and liberates phosphorus. Sudden introduction of P_2S_5-TOP to copper nanocrystals in hot OLA immediately reduces the red phosphorus and induces the reaction between copper and phosphorus. Thiourea acts as a sulfur source when heated in the presence of Cu_3P, leading to the formation of Cu_3PS_4.

Scheme 1. Synthesis of Cu_3P and Cu_3PS_4

1) $P_2S_5 + 5\ TOP \rightarrow 5\ TOPS + 2\ P^*$
2) $Cu(acac)_2 \rightarrow Cu$ (in OLA)
3) $3\ Cu + P^* \rightarrow Cu_3P$
4) $Cu_3P + THU + \Delta \rightarrow Cu_3PS_4$

P^* represents a reactive phosphorus phase.

CONCLUSIONS

We have presented the solution-based synthesis of Cu_3PS_4 from Cu_3P utilizing an in-situ synthesis of amorphous red phosphorus from P_2S_5 and TOP in one pot, followed by sulfurization via the thermal decomposition of thiourea. We have shown that Cu_3P can be synthesized at temperatures between 200 °C and 300 °C with no copper impurities present. The Cu_3P nanocrystals have an increased concentration of phosphorus on their surface, which is caused largely by unreacted amorphous red phosphorus which accounts for the off-stoichiometries routinely observed in EDS analysis. By reacting Cu_3P with sulfur from thermally decomposing thiourea, we have synthesized Cu_3PS_4 in a solution-based process. The effective optical bandgap of p-type Cu_3PS_4 has been experimentally determined to be 2.36 eV, and a photo-generated current density of 3 $\mu A/cm^2$ was observed via PEC measurements, thus showing the potential application of this material as a photo-absorber. The presented synthesis mechanism demonstrates the synthesis and application of one solution-based metal-phosphorus-sulfide alternative energy material, and creates the possibility for further understanding similar earth abundant alternative energy materials.

ACKNOWLEDGEMENTS

The authors would like to give special thanks to Karl Wood for his mass spectrometry assistance, and James Meyer for his experimental assistance. This work was supported by the National Science Foundation's Solar Economy IGERT grant #0903670. E.A.S. acknowledges support from the U.S. DOE Office of Science Facility at Brookhaven National Laboratory under contract No. DE-SC0012704.

REFERENCES

1 S. L. Brock and K. Senevirathne, *J. Solid State Chem.*, 2008, **181**, 1552–1559.

2 S. T. Oyama, T. Gott, H. Zhao and Y.-K. Lee, *Catal. Today*, 2009, **143**, 94–107.

3 J. Wang, Q. Yang, Z. Zhang, T. Li and S. Zhang, *Dalt. Trans.*, 2010, **39**, 227–233.

4 H. Pfeiffer, F. Tancret and T. Brousse, *Electrochim. Acta*, 2005, **50**, 4763–4770.

5 M. C. Stan, R. Klöpsch, A. Bhaskar, J. Li, S. Passerini and M. Winter, *Adv. Energy Mater.*, 2013, **3**, 231–238.

6 C. Villevieille, F. Robert, P. L. Taberna, L. Bazin, P. Simon and L. Monconduit, *J. Mater. Chem.*, 2008, **18**, 5956.

7 J. A. Aitken, V. Ganzha-Hazen and S. L. Brock, *J. Solid State Chem.*, 2005, **178**, 970–975.

8 Y. Xie, H. L. Su, X. F. Qian, X. M. Liu and Y. T. Qian, *J. Solid State Chem.*, 2000, **91**, 88–91.

9 S. Carenco, Y. Hu, I. Florea, O. Ersen, C. Boissie, N. Me and C. Sanchez, *Chem. Mater.*, 2012, **24**, 4134–4145.

10 J. Park, B. Koo, K. Y. Yoon, Y. Hwang, M. Kang, J.-G. Park and T. Hyeon, *J. Am. Chem. Soc.*, 2005, **127**, 8433–40.

11 A. E. Henkes, Y. Vasquez and R. E. Schaak, *J. Am. Chem. Soc.*, 2007, **129**, 1896–7.

12 A. E. Henkes and R. E. Schaak, *Chem. Mater.*, 2007, **19**, 4234–4242.

13 L. De Trizio, A. Figuerola, L. Manna, A. Genovese, C. George, R. Brescia, Z. Saghi, R. Simonutti, M. Van Huis and A. Falqui, *ACS Nano*, 2012, **6**, 32–41.

14 V. Itthibenchapong, R. S. Kokenyesi, A. J. Ritenour, L. N. Zakharov, S. W. Boettcher, J. F. Wager and D. a. Keszler, *J. Mater. Chem. C*, 2013, **1**, 657.

15 L. Yu, R. S. Kokenyesi, D. A. Keszler and A. Zunger, *Adv. Energy Mater.*, 2013, **3**, 43–48.

16 D. H. Foster, V. Jieratum, R. Kykyneshi, D. a. Keszler and G. Schneider, *Appl. Phys. Lett.*, 2011, **99**, 181903.

17 R. B. Balow, E. J. Sheets, M. M. Abu-Omar and R. Agrawal, *Chem. Mater.*, 2015, **27**, 2290–2293.

18 R. Nitsche and P. Wild, *Mat. Res. Bull.*, 1970, **5**, 419–423.

19 J. V. Marzik, A. K. Hsieh, K. Dwight and A. Wold, *J. Solid State Chem.*, 1983, **49**, 43–50.

20 R. Blachnik, B. Gather and E. Andrae, *J. Therm. Anal.*, 1991, **37**, 1289–1298.

21 H. Andrae, *J. Alloys Compd.*, 1992, **189**, 209–215.

22 A. Pfitzner and S. Reiser, *Zeitschrift für Krist.*, 2002, **217**, 51–54.

23 S. Uk Son, I. Kyu Park, J. Park and T. Hyeon, *Chem. Commun.*, 2004, **1**, 778–9.

24 S. Chen, X. Zhang, Q. Zhang and W. Tan, *Nanoscale Res. Lett.*, 2009, **4**, 1159–1165.

25 X. Hou, X. Zhang, S. Chen, Y. Fang, J. Yan, N. Li and P. Qi, *Appl. Surf. Sci.*, 2011, **257**, 4935–4940.

26 O. Olofsson, *Acta Chem. Scand.*, 1972, **26**, 2777–2787.

27 M. H. Mobarok and J. M. Buriak, *Chem. Mater.*, 2014.

28 L. De Trizio, R. Gaspari, G. Bertoni, I. Kriegel, L. Moretti, F. Scotognella, L. Maserati, Y. Zhang, G. C. Messina, M. Prato, S. Marras, A. Cavalli and L. Manna, *Chem. Mater.*, 2015, **27**, 1120–1128.

29 S. Wang, Q. Gao and J. Wang, *J. Phys. Chem. B*, 2005, **109**, 17281–9.

30 V. P. Timchenko, A. L. Novozhilov and O. A. Slepysheva, *Russ. J. Gen. Chem.*, 2004, **74**, 1046–1050.

31 T. Unold and L. Gütay, in *Advanced Characterization Techniques for Thin Film Solar Cells*, eds. D. Abou-Ras, T. Kirchartz and U. Rau, 2011, pp. 151–175.

CAPTIONS

FIG. 1. XRD spectra of Cu_3P synthesized from the in-situ phosphorous source P_2S_5 in TOP (ref. PDF# 01-071-2261). This Cu_3P is reacted with decomposing thiourea to synthesize Cu_3PS_4 also shown (ref. PDF 01-071-3306).

FIG. 2. (a, b) Bright field TEM images of Cu_3P nanocrystals synthesized by the hot injection of a P_2S_5-TOP solution into a solution charged with $Cu(acac)_2$ in oleylamine. (c) Annular dark field STEM image of two Cu_3P nanocrystals. The solid red line indicates the location of the EELS linescan. (d) STEM EELS linescan showing the precise location of elemental signals for P (green triangles) and Cu (yellow circles) indicating a uniform nanocrystal capped with phosphorus. Note that while the Cu:P ratio is constant within the bulk of the nanoparticle (brightest region), the P signal extends beyond the nanocrystal. (e) Bright field TEM image of Cu_3P nanocrystals with (f) accompanying EFTEM phosphorus map confirming the phosphorus-rich surface.

FIG. 3. (a) XRD scans showing the presence of Cu metal (PDF #4-836) with Cu_3P at Cu:P ratios above 2.75:1 and phase-pure Cu_3P at ratios of 2.6:1 and below. (b) Final Cu:P ratios obtained by SEM EDS are found to be dependent on the initial concentration of P_2S_5 in TOP, indicating that excess phosphorus is needed to obtain pure phase Cu_3P.

FIG. 4. STEM EDS linescan of Cu_3PS_4 particles synthesized from the reaction of Cu_3P in 1-octadecene with decomposing thiourea. The Cu_3PS_4 has a uniform atomic composition qualitatively approaching the desired 3:1:4 Cu:P:S ratio. Data represented is a 5-point moving average.

FIG. 5. Photoluminescence spectrum of Cu_3PS_4 showing the peak photoresponses at 2.36 eV (525 nm) and 2.19 eV (566 nm) near the theoretical optical bandgap of 2.38 eV (521 nm).

FIG. 6. PEC data collected from back illuminating Cu_3PS_4 on ITO coated soda-lime glass using Na_2S (0.5 M, pH 12.0 with HCl) as the electrolyte with an applied bias of -1.15 V vs. Ag/AgCl (4 M KCl). As the electrolyte equilibrates, the current density stabilizes to 3 $\mu A/cm^2$ after 600 s.

ABSTRACT FIGURE

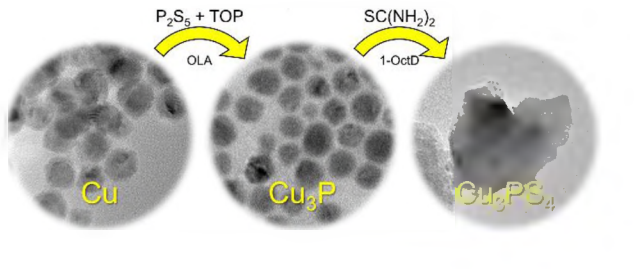

Supplemental Material:

An In-situ Phosphorus Source for the Synthesis of Cu_3P and the Subsequent Conversion to Cu_3PS_4 Nanoparticle Clusters

Erik J. Sheets
School of Chemical Engineering, Purdue University, 480 Stadium Mall Dr. West Lafayette, Indiana 47907, USA

Wei-Chang Yang
School of Materials Engineering, Purdue University, 701 Stadium Mall Dr. West Lafayette, Indiana 47907, USA

Robert B. Balow
Department of Chemistry, Purdue University, 560 Oval Dr. West Lafayette, Indiana 47907, USA

Yunjie Wang and Bryce C. Walker
School of Chemical Engineering, Purdue University, 480 Stadium Mall Dr. West Lafayette, Indiana 47907, USA

Eric A. Stach[a)]
Center for Functional Nanomaterials, Brookhaven National Laboratory, 2 Center Street, Upton, NY 11973, USA

Rakesh Agrawal[b)]
School of Chemical Engineering, Purdue University, 480 Stadium Mall Dr. West Lafayette, Indiana 47907, USA

[a)] This author was an editor of this journal during the review and decision stage. For the *JMR* policy on review and publication of manuscripts authored by editors, please refer to http://www.mrs. org/jmr-editor-manuscripts/

[b)] Address all correspondence to this author. Email: agrawalr@purdue.edu

Characterization Details.

X-ray Diffraction. Samples of both materials were drop cast from ethanol onto a quartz or molybdenum coated glass substrates and were analyzed by x-ray diffraction (XRD) using a Bruker D8 with a Cu-Kα radiation source at room temperature (40 kV, 40 mA). The background was subtracted from the original diffraction patterns without changing peak locations for simple comparisons across multiple scans unless otherwise noted. Molybdenum substrates were used to align the 110 peak to 40.5 degrees 2-theta.

SEM EDS. Field emission scanning electron microscopy energy dispersive x-ray spectroscopy (FE-SEM EDS) measurements were obtained from samples cast onto a silicon wafer substrate using an FEI Quanta 3D FEG Dual-beam scanning electron microscope with an Oxford INCA Xstram-2 silicon drift detector operated at an accelerating voltage of 20 kV. Data analysis was performed using Oxford's INCA software.

TEM. Transmission electron microscopy (TEM) bright field images were obtained using a FEI Technai 20 operated at an accelerating voltage of 200 kV. Scanning TEM (STEM) EDS and STEM electron energy loss spectroscopy (EELS) data was obtained using FEI Titan operated with an accelerating voltage of 300 kV and was analyzed using Oxford's AZTEC software. Samples were cast on holey carbon with 300 mesh Au grids from dilute toluene suspensions. Samples for TEM EDS were prepared on SiN grids. Energy-filtered TEM (EFTEM) was used to detect the small amount of P between the particles as shown in FIG. 2 (e-g). The EFTEM phosphorous map was derived using the three-window method at the P-$L_{2,3}$ edge with a 20 eV energy selecting slit. Two pre-edge images located at 90-110 and 110-130 eV, respectively, were recorded and extrapolated to obtain the background image of a post-edge image at 135-155 eV. The post-edge image was then subtracted by the background image to acquire the phosphorous map.

Photoluminescence Spectroscopy. Photoluminescence spectroscopy (PL) measurements were taken using a Horiba Jobin Yvon T64000 equipped with a 488 nm, 1 mW laser.

GC-MS. Gas chromatography-mass spectroscopy (GC-MS) was used to analyze the intermediate product of P_2S_5 in TOP. An Agilent 5975C mass spectrometer system with a typical electron energy of 70 eV and an ion source temperature of 250 °C was used to analyze dilute samples from toluene. Chemical components were separated using a 30 m DB-5 capillary column with an i.d. of 250 μm and a 0.25 μm film thickness. The initial column temperature was 40 °C which heated to 320 °C at 10 °C/min. The injector temperature was set to 250 °C.

PEC Measurements. Photoelectrodes were fabricated by dropcasting the Cu_3PS_4 on ITO coated soda-lime glass and heating at 200 °C under nitrogen for better adhesion to the substrate. Photoelectrochemical (PEC) measurements were conducted using a Digi-Ivy D2011 single channel potentiostat with a molybdenum counter electrode, Ag/AgCl (4 M KCl) reference electrode, and Cu_3PS_4 nanoparticles on ITO as the working electrode. Solar simulated light at 1 sun intensity (100 mw/cm^2) was used to back-illuminate the Cu_3PS_4 photoelectrodes using a Newport 300 watt Xe arc lamp (Model 66902) with an AM1.5G filter. An infrared (IR) water filter is attached to attenuate the IR light of the solar spectrum to prevent heating of the PEC cell during measurement. The PEC cell was fabricated from fused quartz for transparency to ultraviolet light. To purge the electrolyte, argon was bubbled for at least 1 h prior to PEC measurements. A steady stream of argon was maintained over the quartz cell during PEC measurements.

XRD Refinement. Rietveld refinement of the Cu_3P and Cu_3PS_4 XRD spectrums was done using Maud software. Fitting parameters were attained to verify the goodness of fit. Standard refinement requires Rw < 15 % and Sigma < 2.0. Both refinements are within the acceptable range as seen in TABLE SI below.

TABLE SI. Rietveld refinement parameters for Cu_3P and Cu_3PS_4

	Rw	Sigma
Cu_3P	14.29 %	1.15
Cu_3PS_4	8.72 %	1.88

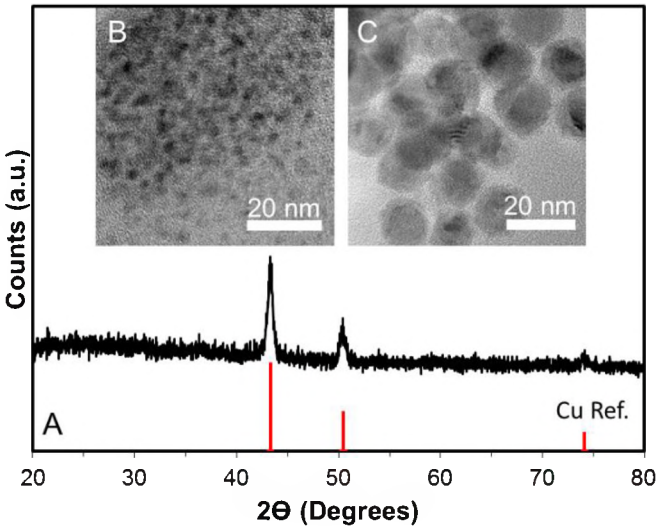

FIG. S1. (A) XRD of copper nanocrystals from copper (II) acetylacetonate in oleylamine with reference to JCPDS# 4-836 (red). (B,C) TEM image of Cu nanocrystals synthesized from $Cu(acac)_2$ in oleylamine at (B) 200 °C, and (C) 300 °C. The average diameter increases from 3.8 nm to 15.0 nm respectively and statistics can be found in FIG. S4.

Copper nanocrystals are formed from copper (II) acetylacetonate (99.99%, Sigma Aldrich) in oleylamine (80-90%, Acros) heated to 300 °C for 30 min under argon in a standard Schlenk line apparatus. Particles were collected and washed in a 1:1 by volume toluene:ethanol solution.

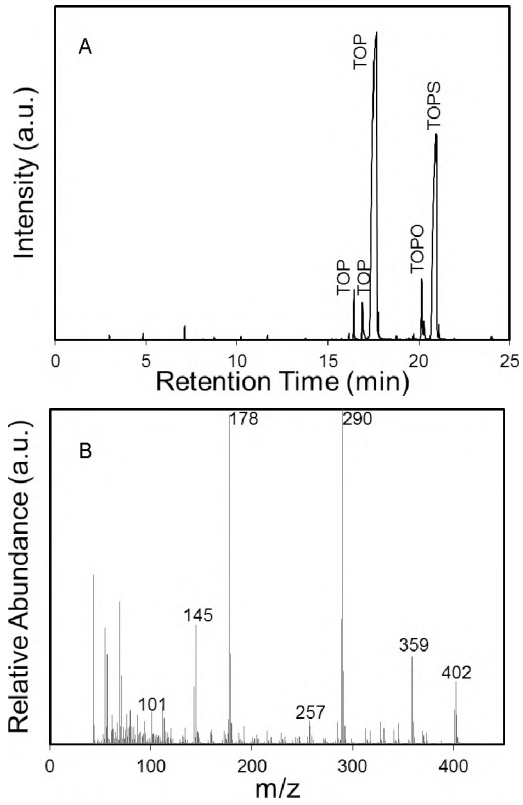

FIG. S2. Gas chromatograph (A) and mass spectrum (B) of P_2S_5 in TOP diluted in toluene confirming the formation of TOPS. The mass spectrum (B) is of the gas phase peak at 21min.

Gas chromatography-mass spectroscopy data of the trioctylphosphine (TOP) and P_2S_5 mixture is depicted in FIG. S2 above. TOP, trioctylphosphine oxide (TOPO), and trioctylphosphine sulfide (TOPS) are observed. The characteristic mass spectrum for TOPS consisting of the main species, m/z 402, and its octyl- groups (C_8H_{17}), m/z 290 and m/z 178, are observed from the mass spectrum of the peak at 21 min. The experiment also indicated an unusual observation of an ion with m/z 359. This indicates the loss of a C_3H_7 ion. The leftover product would then potentially consist of a penthiophane ring attached to the phosphorus atom. The loss of this ring ($C_5H_{10}S$, m/z = 101) would leave an ion with an m/z 257, both of whose m/z are observed. Further, the loss of an octyl- group (C_8H_{17}) from the original de-sulfided phosphorus site would leave an ion consisting of $C_8H_{17}P$ with an m/z of 145, which is observed as well. We

hypothesize the observed breakdown could be related to the McLafferty rearrangement.[1] Regardless, results support the hypothesis that TOP froms TOPS in the presence of P_2S_5.

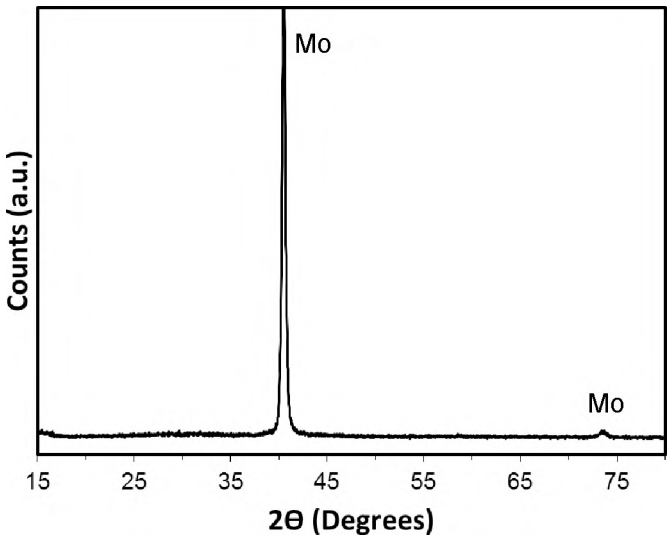

FIG. S3. XRD of amorphous red phosphorus on a molybdenum substrate. No characteristic peaks are observed besides the substrate (molybdenum) peaks. The background was not subtracted from this data.

The TOP-P_2S_5 precursor used in standard Cu_3P syntheses was injected into hot oleylamine (300 °C) without the presence of copper. A red, insoluble precipitate formed which was washed with toluene and cast on a molybdenum coated glass substrate as a reference. XRD in FIG. S3 showed no characteristic peaks other than the substrate. SEM EDS analysis of the precipitate showed a phosphorus:sulfur ratio greater than 100:1. Thus the precipitate was concluded to be amorphous red phosphorus.

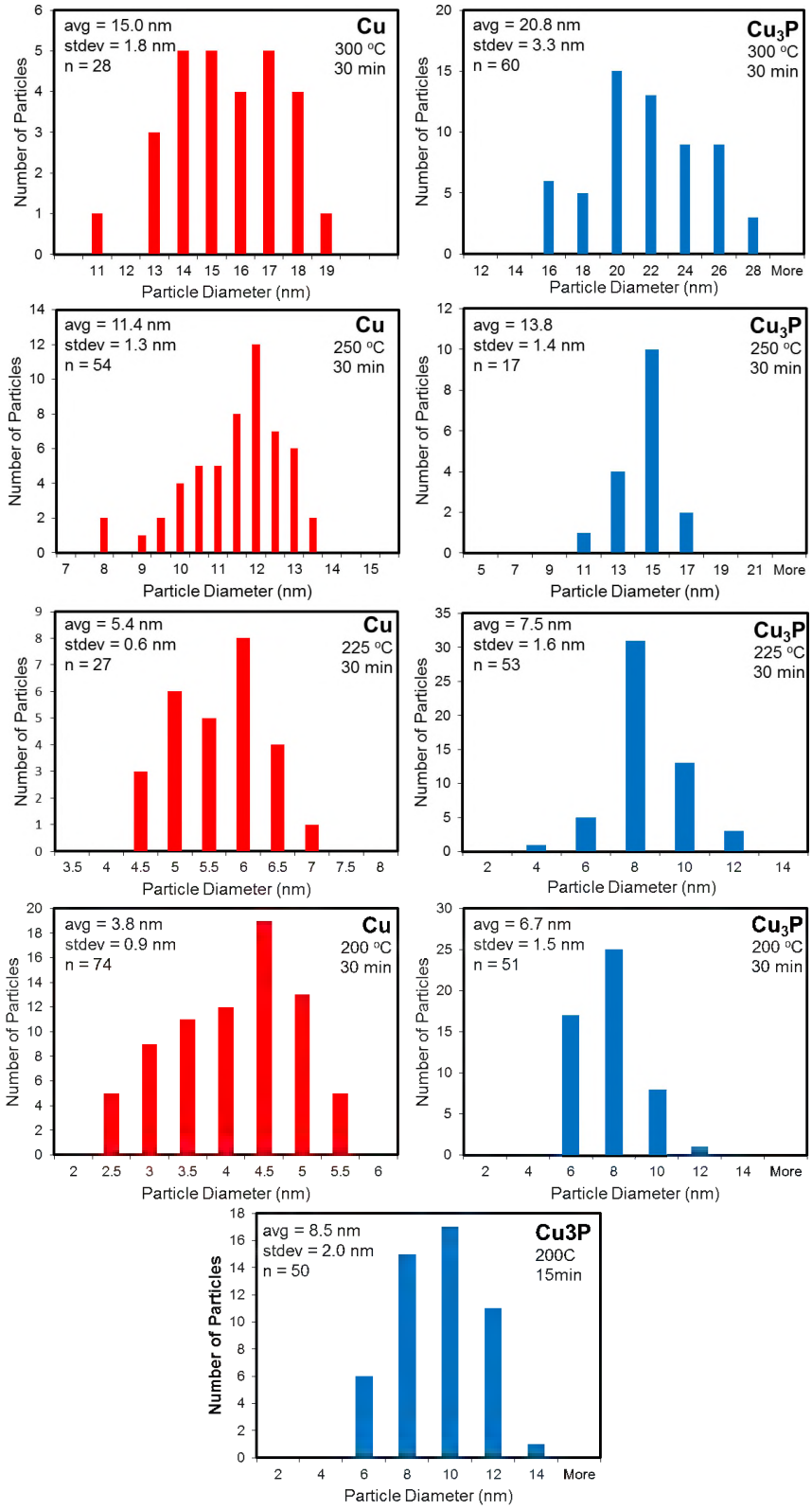

FIG. S4. Particle size distributions for parent copper nanoparticles and as synthesized Cu_3P nanoparticles. Bin sizes on the x-axis represent the maximum size of the particles per bin.

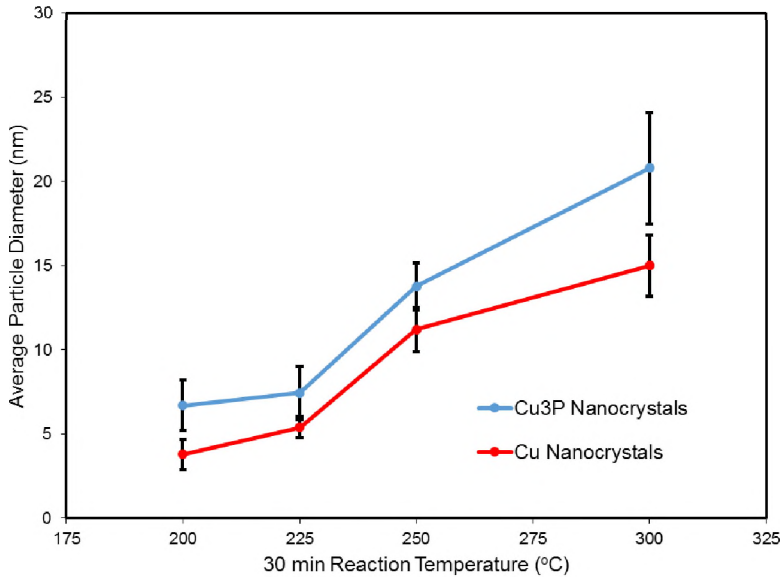

FIG S5. Plot of the average particle diameters and standard deviation (error bars) for the series of experiments observing the growth of copper nanoparticles before their reaction with the P_2S_5-TOP solution at various temperatures.

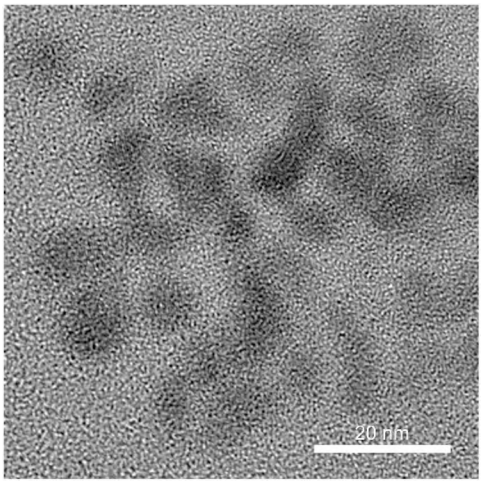

FIG. S6. Cu_3P nanocrystals synthesized at 200 °C are much smaller in comparison to the nanocrystals grown at 300 °C seen in FIG. 2(a).

From FIG. S4-6, we have concluded that the size of the copper nanocrystals initially formed before the injection of the phosphorus source is related to the final size of the Cu_3P nanocrystals. TEM images of copper nanoparticles prior to the injection of the P_2S_5-TOP solution were obtained from removing a small sample (approximately 0.2 mL) at the temperature indicated in FIG S4. Final products after the injection of the P_2S_5-TOP solution were washed and analyzed for particle sizes

for comparison to their copper precursor. Particle diameters were measured by hand using ImageJ software. As temperature increases, so does particle size. A summary of all the data in FIG. S4 is presented as FIG S5.

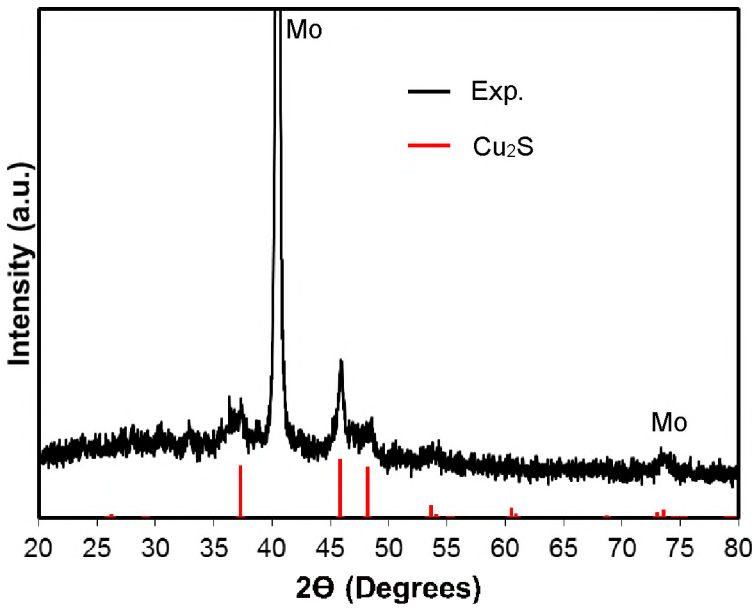

FIG. S7. XRD pattern of the product observed following the reaction of P_2S_5-TOP solution with in-situ formed copper nanocrystals in OLA at 300 °C for 30 min. The minimum molar quantity of TOP was used that would react with all the sulfur from P_2S_5 to observe the effect versus the standard synthesis (excess TOP). Cu_2S was formed (red) (PDS # 53-522).

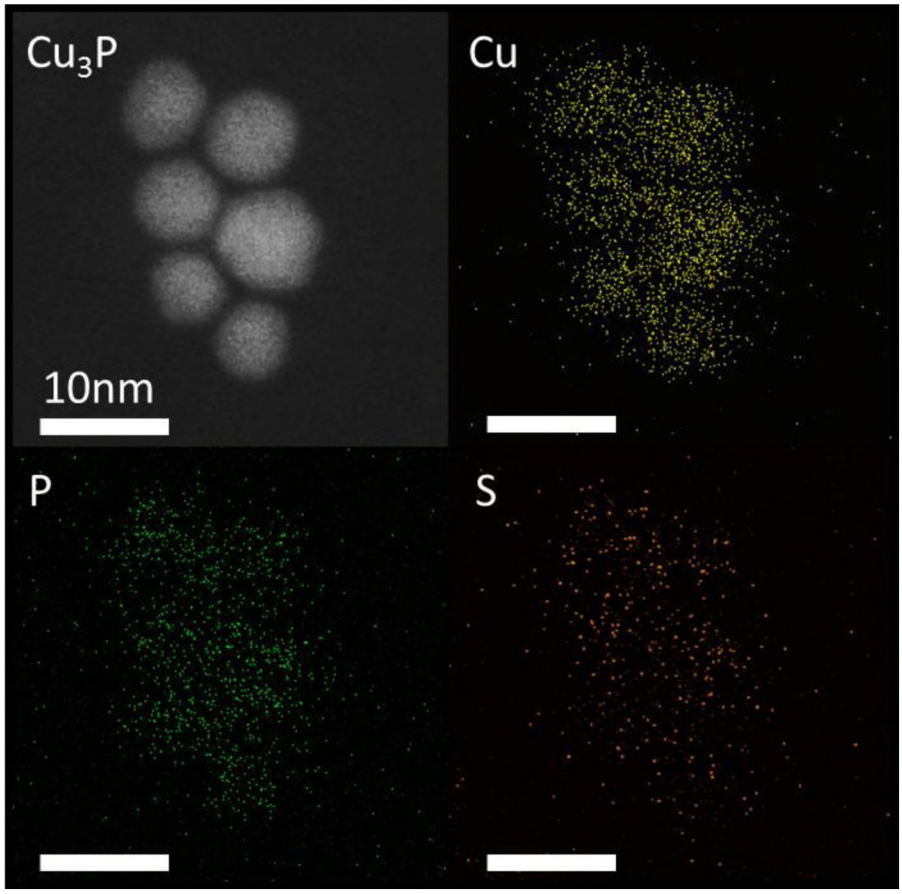

FIG. S8. Dark field STEM image of Cu_3P standard nanocrystals and subsequent elemental maps of Cu, P, and S using EDS.

STEM EDS maps of standard Cu_3P nanocrystals obtained in a 300 kV STEM (FEI Titan) were used to confirm the homogeneity of the synthesized particles. The elemental distributions of Cu and P are found consistent throughout the sample. The weak sulfur signals that coincide with the nanocrystals in the S map are likely due to TOP/TOPS capping ligands on the surface. Compared to that of Cu and P, the signal-to-noise ratio of S map is relatively low and the elemental distribution hardly defines the shapes individual particles. In order to further confirm this, a STEM EDS linescan was performed across the Cu_3P nanocrystals (FIG. S9). In the stacked profile, the copper and phosphorus signals are strong and consistent throughout the particles, while the sulfur signal observed is noisy and weak. On the basis of the EDS results here and the PXRD analysis in

manuscript, the observed S signals are merely contributed to the surface ligands or small amount of solutes in the Cu_3P phase.

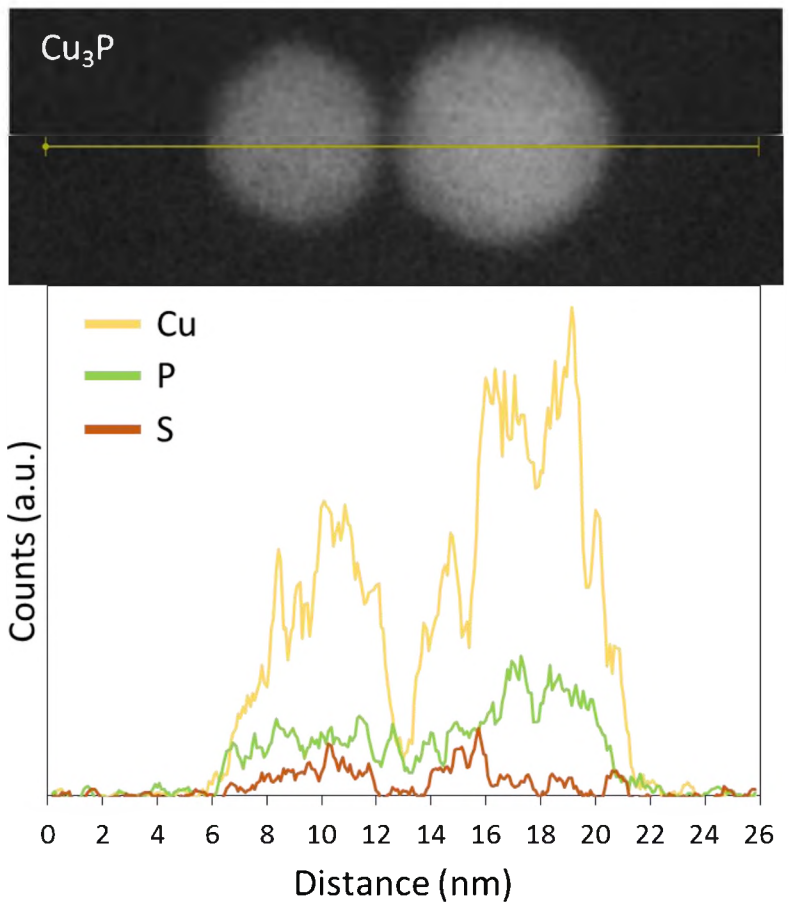

FIG. S9. Dark field STEM image of Cu_3P standard nanocrystals and subsequent elemental linescan of Cu, P, and S using EDS.

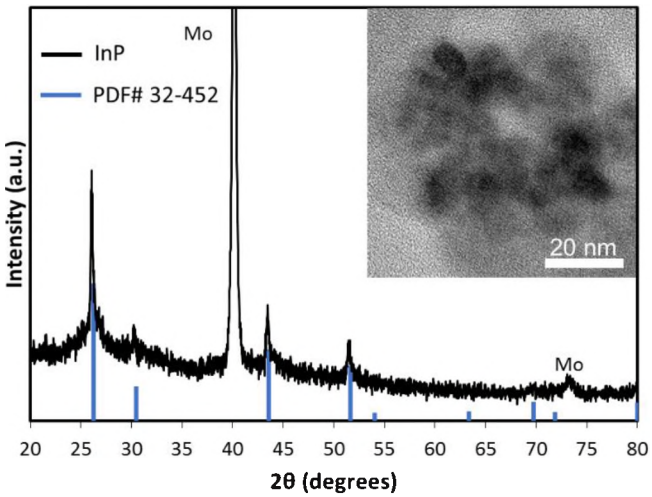

FIG. S10. XRD pattern of InP nanoparticles synthesized by adding 1 mmol $InCl_3$ and 10 ml of 1-octadecene to a flask and heating to 300 °C when a 0.5 mmol solution of P_2S_5 in 4.5 ml TOP is injected. After 2 hours, the product was cooled and washed with toluene and ethanol. InP nanoparticles are drop cast on molybdenum coated soda-lime glass. (inset) Bright field TEM image of an initial InP nanoparticle cluster.

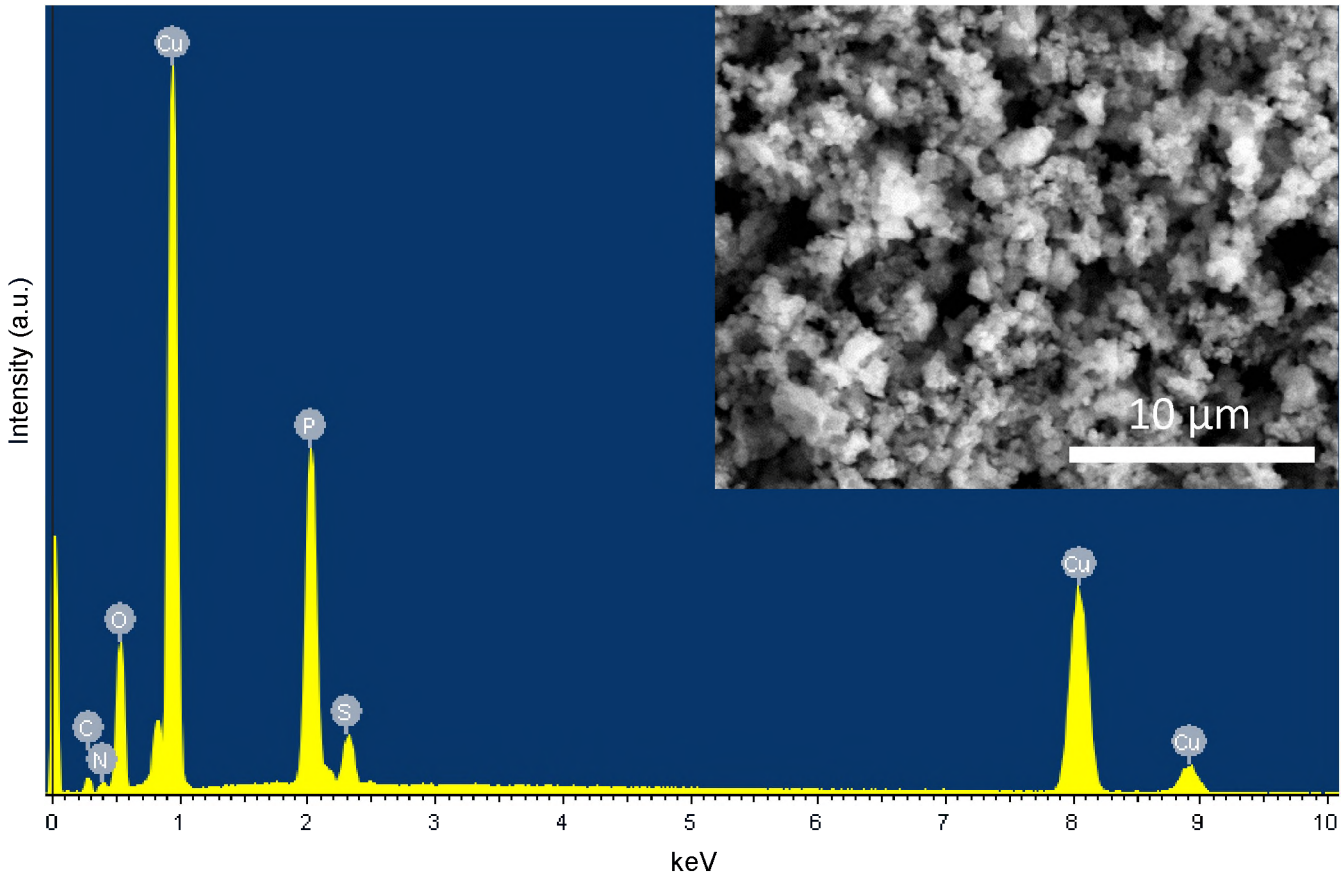

FIG. 11. SEM image and SEM EDS spectra of the Cu_3P nanoparticles as synthesized. Copper and phosphorus dominate the spectrum with a trace of sulfur.

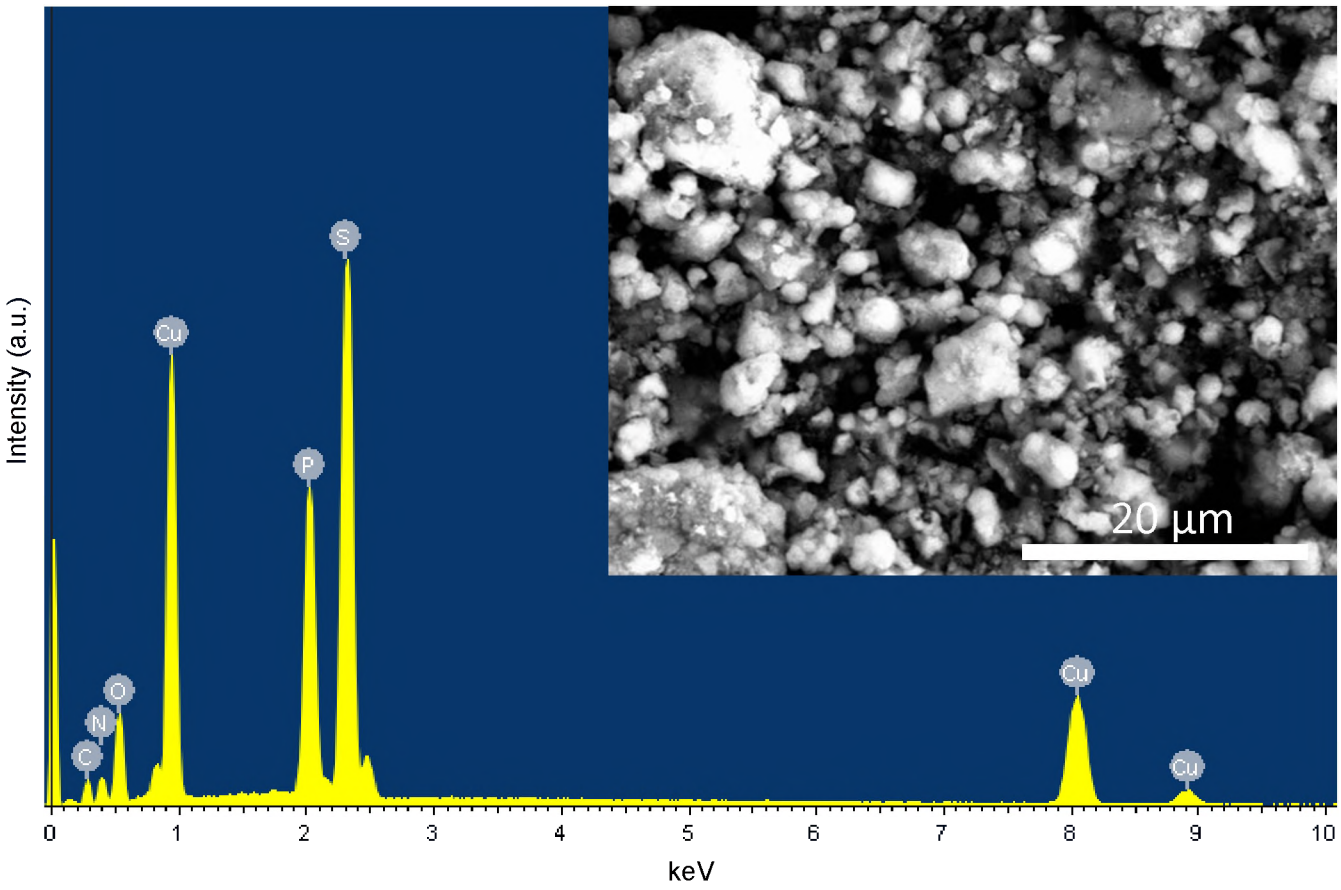

FIG. S12. SEM image and SEM EDS spectra of the Cu_3PS_4 particles using decomposing thiourea in 1-octadecene. Copper, phosphorus, and sulfur are present with an increase in the sulfur conent compared to the original Cu_3P sample.

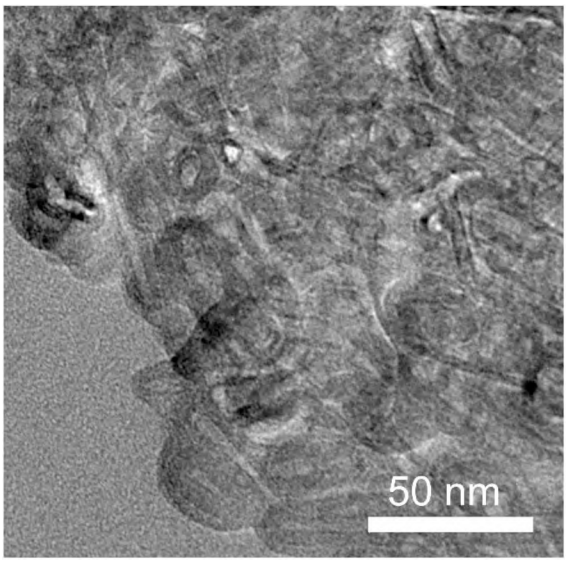

FIG. 13. TEM image of Cu_3PS_4 particles from the reaction of Cu_3P with decomposing thiourea without a solvent present (1-octadecene).

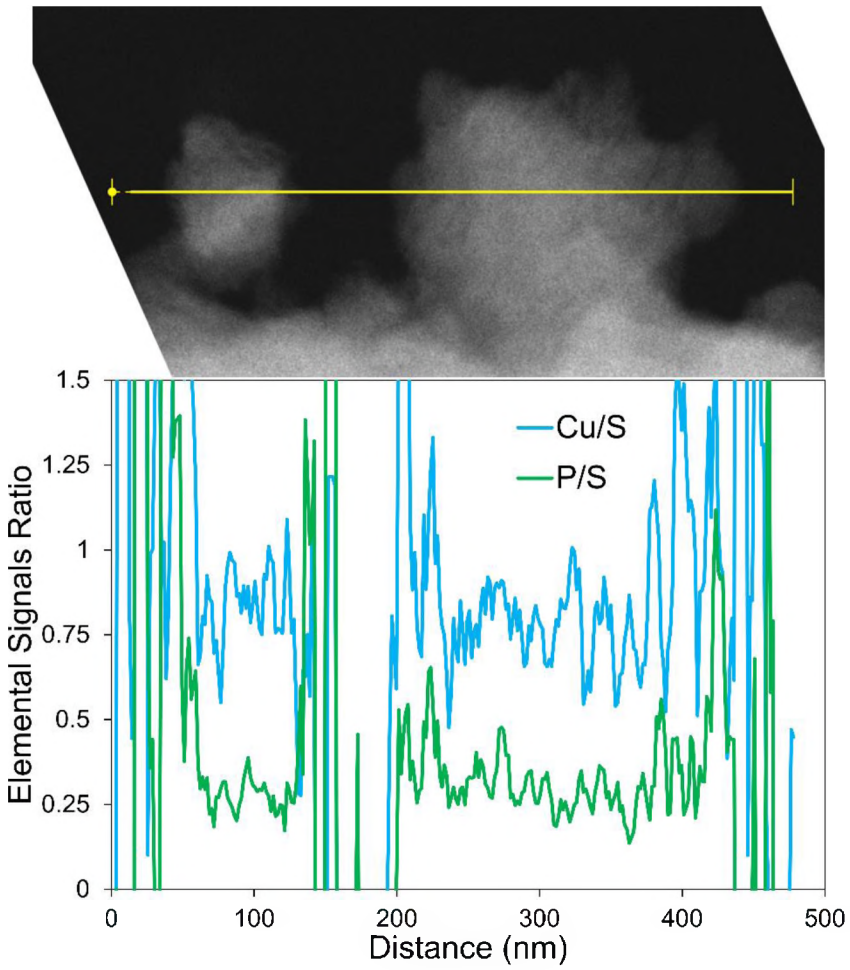

FIG. S14. STEM EDS linescan showing compositional uniformity across the particles by taking the ratio of elemental signals as a function of location (5 point moving average). An effectively flat line is observed in the location of the particles. Near the thin edges of the particles, low detected photon counts cause an increase in the observed noise. Note that the flat ratios (approximately 0.75 and 0.25 for Cu/S and P/S respectively) do not precisely correspond to the compound's overall atomic ratios.